arXiv:1410.3367v2 [hep-ph] 21 Oct 2014

FLAVOUR(267104)-ERC-86
October 22, 2014

News on $B \to K^{(*)}\nu\overline{\nu}$ in the Standard Model and beyond

Jennifer Girrbach-Noe

TUM Institute for Advanced Study
Lichtenbergstr. 2a, 85748 Garching, Germany

An analysis of the rare B decays $B \to K^{(*)}\nu\overline{\nu}$ is presented both within the SM and beyond. The SM predictions for the branching ratios are updated and uncertainties reduced. For the NP analysis both a model independent approach is used and concrete NP models are studied. The relations between $b \to s\nu\overline{\nu}$ and $b \to s\ell^+\ell^-$ transitions are analysed in detail.

PRESENTED AT

Presented at the 8th International Workshop on the CKM Unitarity Triangle (CKM 2014),
Vienna, Austria, September 8-12, 2014

1 Introduction

The decays $B \to K^{(*)}\nu\overline{\nu}$ are theoretically very clean and will play a key role in the tests of the SM and its extensions. They are especially sensitive to Z penguins whereas $b \to s\ell^+\ell^-$ transitions are additionally sensitive to dipole and scalar operators. Due to their sensitivity to right-handed couplings $B \to K^{(*)}\nu\overline{\nu}$ decays offer a powerful test of MFV. This talk is based on [1] and studies $B \to K^{(*)}\nu\overline{\nu}$ both within the SM and beyond. In 2009 these decays were analysed in [2] but since the flavour precision era is ahead of us and due to new lattice calculations and new data on $b \to s\ell^+\ell^-$ transitions it is time to have a closer look at $B \to K^{(*)}\nu\overline{\nu}$ again. The main novelties of [1] are:

- The SM predictions for the branching ratios and the angular observable F_L are updated. Due to new lattice calculations the form factor uncertainties decreased considerably [3, 4].
- We exploit the $\mathrm{SU}(2)_L$ symmetry in order to relate $b \to s\ell^+\ell^-$ and $b \to s\nu\overline{\nu}$ transitions.
- New data on $B \to K^*\mu^+\mu^-$ and its impact on $B \to K^{(*)}\nu\overline{\nu}$ are included.
- We study correlations both in a model-independent approach and in concrete models beyond the SM.
- The impact of lepton flavour non-universality is also discussed in [1] but not covered in this talk.

2 SM results

In the SM only one operator contributes to $B \to K^{(*)}\nu\overline{\nu}$:

$$\mathcal{H}_{\text{eff}}^{\text{SM}} = -\frac{4\,G_F}{\sqrt{2}} V_{tb}V_{ts}^* C_L^{\text{SM}} \mathcal{O}_L \;+\; \text{h.c.}\,, \quad \mathcal{O}_L = \frac{e^2}{16\pi^2}(\overline{s}\gamma_\mu P_L b)(\overline{\nu}\gamma^\mu(1-\gamma_5)\nu) \tag{1a}$$

$$C_L^{\text{SM}} = -X_t/s_w^2\,, \quad X_t = 1.469 \pm 0.017 \tag{1b}$$

and its Wilson coefficient C_L^{SM} is known very precisely (including NLO QCD corrections [5, 6, 7] and two-loop electroweak contributions [8]). The form factors for the exclusive decays $B \to K^{(*)}\nu\overline{\nu}$ have to be calculated by means of non-perturbative methods. Great progress has been made by lattice calculation, especially at large q^2 [3, 4]. At low q^2 the results from light-cone sum rules are used [9, 10]. Further details can be found in [1] and the rescaled form factors are shown there in appendix A.

Our new result for the total branching ratios in the SM and for the K^* longitudinal polarization fraction F_L that update earlier determinations in [2, 11] are given as:

$$\mathrm{BR}(B^+ \to K^+ \nu\overline{\nu})_{\mathrm{SM}} = (4.20 \pm 0.33 \pm 0.15) \times 10^{-6}, \tag{2}$$

$$\mathrm{BR}(B^0 \to K^{*0} \nu\overline{\nu})_{\mathrm{SM}} = (9.93 \pm 0.74 \pm 0.35) \times 10^{-6}, \tag{3}$$

$$F_L^{\mathrm{SM}} = 0.53 \pm 0.05\,, \tag{4}$$

where the first error is due to form factor uncertainties and the second one is parametric and dominated by CKM uncertainties. Our result for $\mathrm{BR}(B^0 \to K^{*0}\nu\overline{\nu})_{\mathrm{SM}}$ is roughly 40% higher than the one presented in [2] (for further details see [1]). These numbers should be compared with the current experimental upper bounds. BaBar finds the following upper bound [12]:

$$\mathrm{BR}(B^+ \to K^+ \nu\overline{\nu}) < 1.7 \times 10^{-5}\ (90\%\ \mathrm{CL}). \tag{5}$$

Belle has the strongest bound on the $B \to K^*\nu\overline{\nu}$ [13]:

$$\mathrm{BR}(B^0 \to K^{*0} \nu\overline{\nu}) < 5.5 \times 10^{-5}\ (90\%\ \mathrm{CL}), \tag{6}$$

$$\mathrm{BR}(B^+ \to K^{*+} \nu\overline{\nu}) < 4.0 \times 10^{-5}\ (90\%\ \mathrm{CL}). \tag{7}$$

Thus, currently the experimental bounds are roughly a factor of four larger than the SM predictions.

3 Going beyond the SM

3.1 Effective field theory approach

If we go beyond the SM there is one additional operator at low energy, namely $\mathcal{O}_R^\ell = \frac{e^2}{16\pi^2}(\overline{s}\gamma_\mu P_R b)(\overline{\nu}_\ell \gamma^\mu(1-\gamma_5)\nu_\ell)$ with $\ell = e, \mu, \tau$. To be more general we distinguish here between the different lepton flavours. Denoting C_R^ℓ the corresponding Wilson coefficient and analogously C_L^ℓ we define

$$\epsilon_\ell = \frac{\sqrt{|C_L^\ell|^2 + |C_R^\ell|^2}}{|C_L^{\mathrm{SM}}|} \qquad \eta_\ell = \frac{-\mathrm{Re}\left(C_L^\ell C_R^{\ell *}\right)}{|C_L^\ell|^2 + |C_R^\ell|^2} \tag{8}$$

with $\epsilon_\ell = 1$ and $\eta_\ell = 0$ in the SM. The changes with respect to the SM results depend only on these two quantities and can be expressed as follows:

$$\mathcal{R}_K \equiv \frac{\mathcal{B}_K}{\mathcal{B}_K^{\mathrm{SM}}} = \frac{1}{3}\sum_\ell (1 - 2\,\eta_\ell)\epsilon_\ell^2 \quad \xrightarrow{\mathrm{LFU}} \quad (1 - 2\,\eta)\epsilon^2\,, \tag{9}$$

$$\mathcal{R}_{K^*} \equiv \frac{\mathcal{B}_{K^*}}{\mathcal{B}_{K^*}^{\mathrm{SM}}} = \frac{1}{3}\sum_\ell (1 + \kappa_\eta \eta_\ell)\epsilon_\ell^2 \quad \xrightarrow{\mathrm{LFU}} \quad (1 + \kappa_\eta \eta)\epsilon^2\,, \tag{10}$$

$$\mathcal{R}_{F_L} \equiv \frac{F_L}{F_L^{\mathrm{SM}}} = \frac{\sum_\ell \epsilon_\ell^2(1 + 2\,\eta_\ell)}{\sum_\ell \epsilon_\ell^2(1 + \kappa_\eta \eta_\ell)} \quad \xrightarrow{\mathrm{LFU}} \quad \frac{1 + 2\eta}{1 + \kappa_\eta \eta}\,. \tag{11}$$

model	$\widetilde{c}_Z$	$\widetilde{c}^{(1)}_{q\ell}$	$\widetilde{c}^{(3)}_{q\ell}$	$\widetilde{c}_{qe}$	$\widetilde{c}'_Z$	$\widetilde{c}_{de}$	$\widetilde{c}_{d\ell}$
MFV, $U(2)^3$	x	x	x	x	-	-	-
MSSM	x	-	-	-	-	-	-
Part. comp.: bidoublet	x	-	-	-	-	-	-
Part. comp.: triplet	-	-	-	-	x	-	-
331 model	x	x	-	x	-	-	-
general Z' model	-	x	-	x	-	x	x

Table 1: Wilson coefficients that are sizable (x) and negligible/zero (-) in different NP models.

Here we also show what happens in case of lepton flavour universality (LFU). As one can see these observables are very sensitive to right-handed currents and are thus a powerful test of MFV.

In order to exploit the $\mathrm{SU}(2)_L$ symmetry that connects left-handed charged leptons and neutrinos we list here all relevant dimension-6 operators that are invariant under the SM gauge group $\mathrm{G_{SM}}$ that contribute to both $b \to s\ell^+\ell^-$ and $b \to s\nu\overline{\nu}$ transitions [14, 15]*:

$$Q^{(1)}_{Hq} = i(\overline{q}_L\gamma_\mu q_L)H^\dagger D^\mu H\,, \qquad Q^{(1)}_{q\ell} = (\overline{q}_L\gamma_\mu q_L)(\overline{\ell}_L\gamma^\mu \ell_L)\,, \tag{12a}$$

$$Q^{(3)}_{Hq} = i(\overline{q}_L\gamma_\mu \tau^a q_L)H^\dagger D^\mu \tau_a H\,, \qquad Q^{(3)}_{q\ell} = (\overline{q}_L\gamma_\mu \tau^a q_L)(\overline{\ell}_L\gamma^\mu \tau_a \ell_L)\,, \tag{12b}$$

$$Q_{Hd} = i(\overline{d}_R\gamma_\mu d_R)H^\dagger D^\mu H\,, \qquad Q_{d\ell} = (\overline{d}_R\gamma_\mu d_R)(\overline{\ell}_L\gamma^\mu \ell_L) \tag{12c}$$

Furthermore we need to consider those that contribute only to $b \to s\ell^+\ell^-$ but not to $b \to s\nu\overline{\nu}$:

$$Q_{de} = (\overline{d}_R\gamma_\mu d_R)(\overline{e}_R\gamma^\mu e_R)\,, \qquad Q_{qe} = (\overline{q}_L\gamma_\mu q_L)(\overline{e}_R\gamma^\mu e_R)\,. \tag{13}$$

The corresponding Wilson coefficients are denoted as $c^{(1)}_{q\ell}$ etc. We do not include dipole and scalar operators here for simplicity. Dipole operators are only relevant at low q^2 and scalar operators only in $B_s \to \mu^+\mu^-$.

After electroweak symmetry breaking these Wilson coefficients can be mapped onto the basis of the usual $\Delta F = 1$ operators. With a proper choice of normalization

*Such an EFT approach has recently received increasing interest in flavour physics, see e.g. [16, 17, 18].

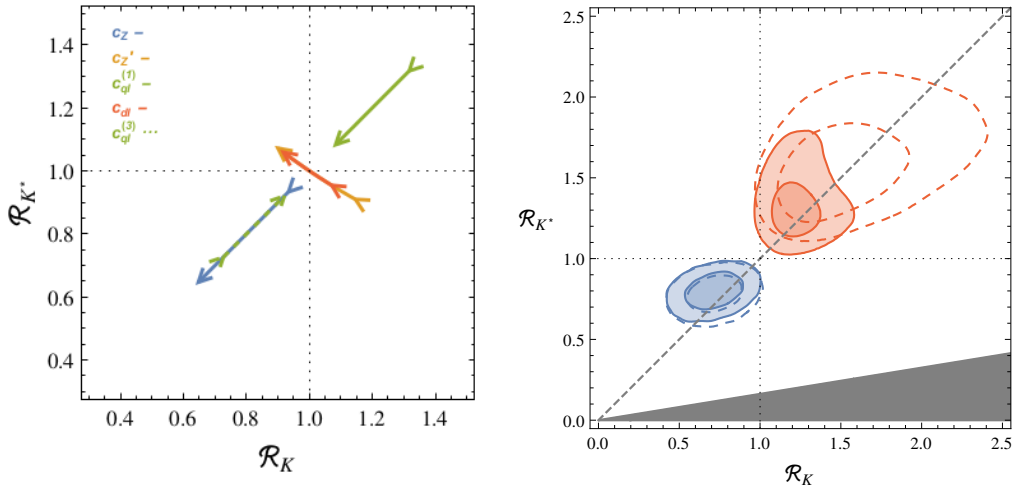

Figure 1: Correlation between $\mathcal{R}^*$ and $\mathcal{R}$. Left: only one Wilson coefficient is non-zero (blue: $\tilde{c}_Z$, yellow: $\tilde{c}'_Z$, green: $\tilde{c}^{(1)}_{ql}$ (solid) or $\tilde{c}^{(3)}_{ql}$ (dashed), red: $\tilde{c}_{dl}$). Right: only Z penguins, i.e. $\widetilde{c}_Z$ and $\widetilde{c}'_Z$ (blue) and only 4-fermion operators, i.e. $c^{(1)}_{ql}$, c_{qe}, $c_{d\ell}$, c_{de} (red) with real (solid) or complex (dashed) Wilson coefficients, respectively.

we get (for details see [1]):

$$B \to K^{(*)}\nu\overline{\nu}: \quad C_L = C_L^{\rm SM} + \widetilde{c}^{(1)}_{q\ell} - \widetilde{c}^{(3)}_{q\ell} + \widetilde{c}_Z\,, \qquad C_R = \widetilde{c}_{d\ell} + \widetilde{c}'_Z\,, \tag{14}$$

$$B \to K^{(*)}\ell^+\ell^-: \quad C_9 = C_9^{\rm SM} + \widetilde{c}_{qe} + \widetilde{c}^{(1)}_{q\ell} + \widetilde{c}^{(3)}_{q\ell} - \zeta\,\widetilde{c}_Z\,, \quad C'_9 = \widetilde{c}_{de} + \widetilde{c}_{d\ell} - \zeta\,\widetilde{c}'_Z\,, \tag{15}$$

$$B_s \to \mu^+\mu^-: \quad C_{10} = C_{10}^{\rm SM} + \widetilde{c}_{qe} - \widetilde{c}^{(1)}_{q\ell} - \widetilde{c}^{(3)}_{q\ell} + \widetilde{c}_Z\,, \quad C'_{10} = \widetilde{c}_{de} - \widetilde{c}_{d\ell} + \widetilde{c}'_Z \tag{16}$$

In complete generality, NP effects in $b \to s\nu\overline{\nu}$ cannot be constrained by $b \to s\ell^+\ell^-$. However in most models not all operators appear and thus only a subset of Wilson coefficients are non-zero. In tab. 1 we summarize which Wilson coefficients can appear in different NP models.

In our numerical analysis we include bounds from $b \to s\ell^+\ell^-$ transitions that mainly constrain $C^{(\prime)}_{9,10}$ using a global numerical analysis from [19, 20, 21, 22]†. Since this is based on data from $b \to s\mu^+\mu^-$ transitions the bounds change in case of lepton flavour non-universality. On the left-hand side of fig. 1 we show the correlation between $\mathcal{R}^*$ and $\mathcal{R}$ where only one Wilson coefficient is non-zero. The coloured arrows correspond to the 2σ allowed ranges of the $b \to s\mu^+\mu^-$ data, with the direction of the arrow pointing from negative to positive values for the $\tilde{c}_i$. On the right-hand side we show the result where we assume NP only in Z penguins, thus $\widetilde{c}_Z$ and $\widetilde{c}'_Z$ are non-zero (blue) and where NP only appears in 4-fermion operators (red), corresponding to a Z'

†Similar global analyses have been performed in [23, 24]. An analysis of $B \to K^*\ell^+\ell^-$ in Randall Sundrum was performed in [25].

model. It is interesting to note that $B \to K^{(*)}\nu\overline{\nu}$ are both enhanced for Z' and both suppressed for Z which makes it possible to distinguish between those two scenarios.

3.2 Concrete NP models

Here we sketch our results in concrete NP models: Z' models, 331 model, MSSM and Partial Compositeness. Leptoquark models and the case of lepton flavour non-universality are not covered in this talk but can be found in [1][‡].

3.2.1 General Z' models

We will first study general Z' models as discussed in detail in [27, 28, 29]. We assume that NP contributions are dominated by the tree-level exchange of a Z' that transforms as a singlet under $SU(2)_L$. We distinguish here between four different scenarios in which only LH quark couplings are present (LHS, red), the one with only RH couplings (RHS, blue), the one with LH and RH couplings being equal (LRS, green) and one with these couplings differing by sign (ALR, yellow). In fig. 2 we show the result for several correlations defining

$$\mathcal{R}_{\mu\mu} = \frac{\mathrm{BR}(B_s \to \mu^+\mu^-)}{\mathrm{BR}(B_s \to \mu^+\mu^-)_{\mathrm{SM}}}\,, \tag{17}$$

$$\mathcal{R}_{K\mu\mu} = \frac{\mathrm{BR}(B^+ \to K^+\mu^+\mu^-)^{[15,22]}}{\mathrm{BR}(B^+ \to K^+\mu^+\mu^-)^{[15,22]}_{\mathrm{SM}}}\,, \quad \mathcal{R}_{K^*\mu\mu} = \frac{\mathrm{BR}(B^0 \to K^{*0}\mu^+\mu^-)^{[15,19]}}{\mathrm{BR}(B^0 \to K^{*0}\mu^+\mu^-)^{[15,19]}_{\mathrm{SM}}}\,, \tag{18}$$

where constraints from $\Delta F = 2$ observables and $b \to s\mu^+\mu^-$ constraints are included. Interestingly, the present suppressions in the data in $B_s \to \mu^+\mu^-$, $B \to K^{(*)}\mu^+\mu^-$ favour left-handed currents that can be explained by Z (tree or penguins) and Z'. As shown in fig. 1 $B \to K^{(*)}\nu\overline{\nu}$ can distinguish these two mechanisms. Using the DNA charts in [31] a qualitative understanding of these plots can be gained.

3.2.2 331 models

The 331 model is based on the symmetry group $SU(3)_C \times SU(3)_L \times U(1)_X$ and is a concrete realization of a Z' model. A nice theoretical feature of this model is that there is an explanation of why there are exactly three generations. This follows from anomaly cancellation and asymptotic freedom of QCD. In the 331 model the Z' has flavour changing left-handed quark currents at tree level while right-handed currents are flavour conserving. Consequently we have $\mathcal{R}^\star = \mathcal{R}$. Due to $Z' - Z$ mixing also Z flavour changing couplings at tree level are induced. Details on the model can be found in [30, 32, 33]. The relevant Wilson coefficients are $\widetilde{c}_Z$, $\widetilde{c}^{(1)}_{ql}$ and

[‡]A recent study of $b \to s\nu\overline{\nu}$ transitions in RS_c models can be found in [26].

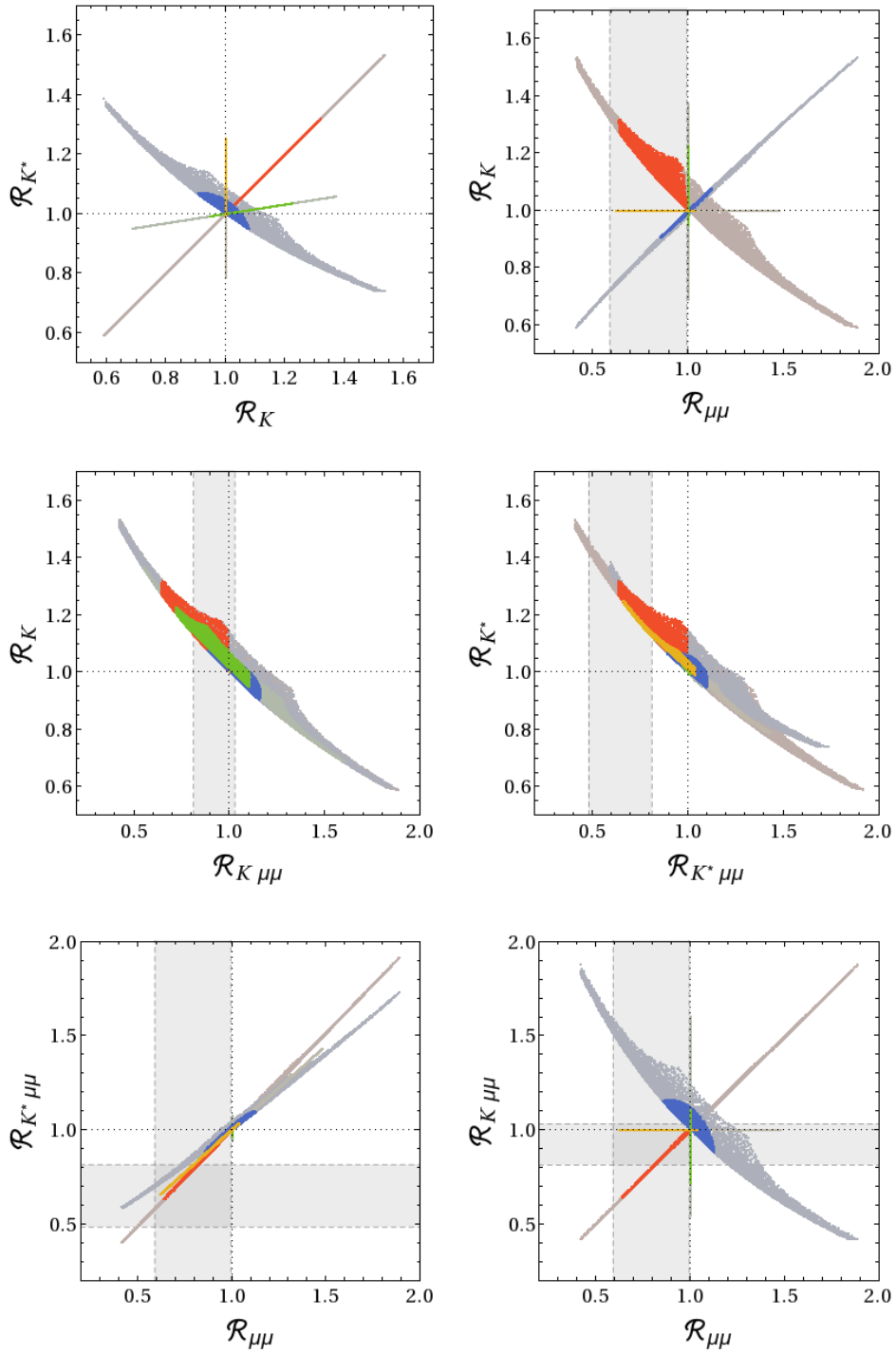

Figure 2: Various correlations between observables in LHS (red), RHS (blue), LRS (green), ALRS (yellow), assuming LFU and $\Delta_R^{\nu\nu} = \Delta_R^{\ell\ell} = 0$. All points satisfy $0.9 \leq C_{B_s} \leq 1.1$, $-0.14 \leq S_{\psi\phi} \leq 0.14$. Grey regions are disfavoured at 2σ by $b \to s\mu^+\mu^-$ constraints.

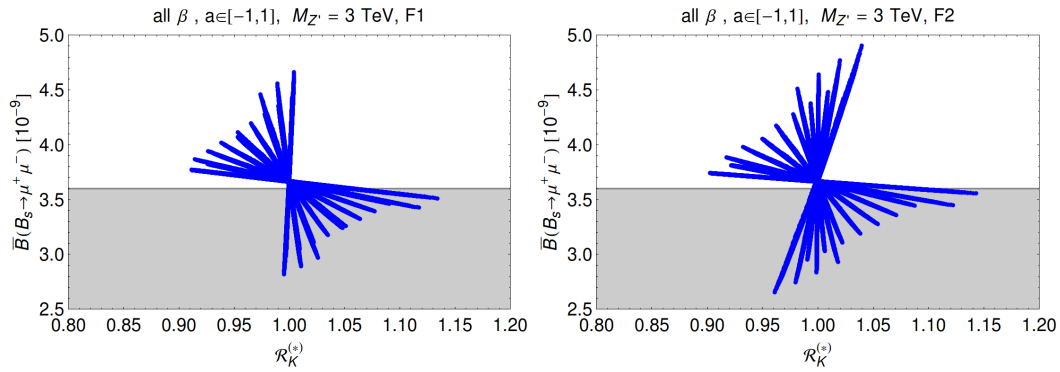

Figure 3: Correlation $\overline{\text{BR}}(B_s \to \mu^+\mu^-)$ versus $\mathcal{R}_K^{(*)}$ in the 331 model for $M_{Z'} = 3$ TeV for fermion representations F1 (left) and F2 (right).

$\widetilde{c}_{qe}$ with $\widetilde{c}_{q\ell}^{(1)} \propto \widetilde{c}_Z$. There are several different versions of 331 models depending on the parameter β that determines the charge operator. In fig. 3 we scanned over many different versions and show the possible range in the $\overline{\text{BR}}(B_s \to \mu^+\mu^-) - \mathcal{R}_K$ region for the two different fermion representations that are possible in 331 models. Constraints from $\Delta F = 2$ observables (ΔM_s and $S_{\psi\phi}$) and from $b \to s\mu^+\mu^-$ transitions are included as well as bounds from electroweak precision observables. Since $\widetilde{c}_{qe} + \widetilde{c}_{q\ell}^{(1)}$ enters C_9 while $\widetilde{c}_{qe} - \widetilde{c}_{q\ell}^{(1)}$ enters C_{10} it is difficult to get large effects in $B_d \to K^*\mu^+\mu^-$ and $B_s \to \mu^+\mu^-$ simultaneously. A suppression of $B_s \to \mu^+\mu^-$, as favoured by present data, almost always implies an enhancement of $\mathcal{R}_K$, but at most by 15%. Models where both are enhanced or suppressed simultaneously are excluded due to constraints from electroweak observables.

3.2.3 MSSM

In the MSSM the dominant effects arise from Z penguins, thus $\widetilde{c}_Z$ (only large in non-MFV) and $\widetilde{c}'_Z$ (small due to constraints from $\text{BR}(B_s \to \mu^+\mu^-)$). The result of our parameter scan is shown in fig. 4 (left). In our scan LHC bounds on sparticle masses are included using `FastLim 1.0` [34], the lightest neutralino is the LSP, `SUSY_FLAVOR` [35] is used to impose FCNC constraints and the lightest Higgs mass is computed with `SPheno 3.3.2` [36, 37]. As one can see RH currents are small in the MSSM, so that $\mathcal{R}_K \approx \mathcal{R}_{K^*}$ and $B \to K^{(*)}\nu\overline{\nu}$ are at most 30% enhanced or suppressed.

3.2.4 Partial Compositeness

A simple model with partial compositeness was analysed in [38] where the dominant contribution to $b \to s\nu\overline{\nu}$ transitions come from tree-level flavour-changing Z couplings. In the "bidoublet model" $\widetilde{c}_Z$ has the largest effect and $\widetilde{c}'_Z$ in the "triplet

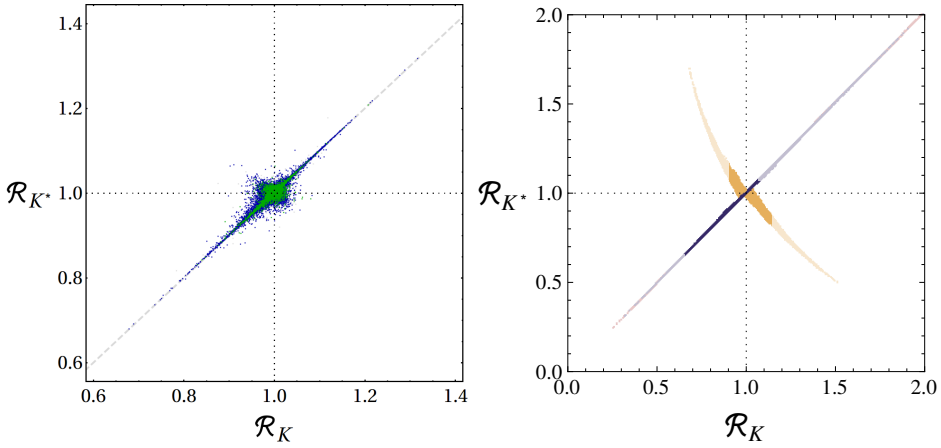

Figure 4: Left: Allowed ranges for $\mathcal{R}^\star$ and $\mathcal{R}$ in the MSSM. All dark points pass flavour and collider constraints; black points have the corrected lightest Higgs mass. Right: Allowed ranges in models with partial compositeness, for two different choices of fermion representations: bidoublet model (blue), triplet model (yellow). Light points are disfavoured at 2σ by $b \to s\mu^+\mu^-$ data. Plot adapted from [38].

model". The results of these two models are shown on the right hand side of fig. 4.

4 Summary

We analysed $b \to s\nu\overline{\nu}$ transitions within the SM and beyond. Due to reduced form factor uncertainties our updated SM predictions have smaller errors of about 10% and are also more reliable. $\mathrm{BR}(B \to K^*\nu\overline{\nu})_{\mathrm{SM}}$ is found to be by 40% larger than previous estimates. Using the $\mathrm{SU}(2)_L$ symmetry we correlate $b \to s\nu\overline{\nu}$ and $b \to s\ell^+\ell^-$ and impose the constraints by recent measurements of $b \to s\mu^+\mu^-$ transition on $B \to K^{(*)}\nu\overline{\nu}$. This limits the relative deviations from the SM to roughly $\pm 60\%$ and in case of lepton flavour non-universality if NP only affects muons, the effects are at most $\pm 20\%$. We find that $b \to s\nu\overline{\nu}$ gives complementary information to NP in $b \to s\ell^+\ell^-$ and can help to disentangle possible NP dynamics behind the anomalies in $B \to K^{(*)}\mu^+\mu^-$.

ACKNOWLEDGEMENTS

I thank the organisers for the opportunity to give this talk and my collaborators A. J. Buras, C. Niehoff and D. Straub for an enjoyable collaboration. I thank Andrzej Buras and David Straub for proofreading this manuscript. I acknowledge financial support by ERC Advanced Grant project "FLAVOUR" (267104).

References

[1] A. J. Buras, J. Girrbach-Noe, C. Niehoff and D. M. Straub, arXiv:1409.4557 [hep-ph].

[2] W. Altmannshofer, A. J. Buras, D. M. Straub and M. Wick, JHEP **0904** (2009) 022 [arXiv:0902.0160 [hep-ph]].

[3] C. Bouchard *et al.* [HPQCD Collaboration], Phys. Rev. D **88** (2013) 5, 054509 [Erratum-ibid. D **88** (2013) 7, 079901] [arXiv:1306.2384 [hep-lat]].

[4] R. R. Horgan, Z. Liu, S. Meinel and M. Wingate, Phys. Rev. D **89** (2014) 094501 [arXiv:1310.3722 [hep-lat]].

[5] G. Buchalla and A. J. Buras, Nucl. Phys. B **400** (1993) 225.

[6] M. Misiak and J. Urban, Phys. Lett. B **451** (1999) 161 [hep-ph/9901278].

[7] G. Buchalla and A. J. Buras, Nucl. Phys. B **548** (1999) 309 [hep-ph/9901288].

[8] J. Brod, M. Gorbahn and E. Stamou, Phys. Rev. D **83** (2011) 034030 [arXiv:1009.0947 [hep-ph]].

[9] P. Ball and R. Zwicky, Phys. Rev. D **71** (2005) 014015 [hep-ph/0406232].

[10] P. Ball and R. Zwicky, Phys. Rev. D **71** (2005) 014029 [hep-ph/0412079].

[11] M. Bartsch, M. Beylich, G. Buchalla and D.-N. Gao, JHEP **0911** (2009) 011 [arXiv:0909.1512 [hep-ph]].

[12] J. P. Lees *et al.* [BaBar Collaboration], Phys. Rev. D **87** (2013) 11, 112005 [arXiv:1303.7465 [hep-ex]].

[13] O. Lutz *et al.* [Belle Collaboration], Phys. Rev. D **87** (2013) 11, 111103 [arXiv:1303.3719 [hep-ex]].

[14] W. Buchmuller and D. Wyler, Nucl. Phys. B **268** (1986) 621.

[15] B. Grzadkowski, M. Iskrzynski, M. Misiak and J. Rosiek, JHEP **1010** (2010) 085 [arXiv:1008.4884 [hep-ph]].

[16] A. Crivellin and S. Pokorski, arXiv:1407.1320 [hep-ph].

[17] R. Alonso, B. Grinstein and J. M. Camalich, arXiv:1407.7044 [hep-ph].

[18] G. Hiller and M. Schmaltz, Phys. Rev. D **90** (2014) 054014 [arXiv:1408.1627 [hep-ph]].

[19] W. Altmannshofer, P. Paradisi and D. M. Straub, JHEP **1204** (2012) 008 [arXiv:1111.1257 [hep-ph]].

[20] W. Altmannshofer and D. M. Straub, Eur. Phys. J. C **73** (2013) 2646 [arXiv:1308.1501 [hep-ph]].

[21] W. Altmannshofer and D. M. Straub, in preparation

[22] W. Altmannshofer talk given at CKM 2014

[23] S. Descotes-Genon, J. Matias and J. Virto, Phys. Rev. D **88** (2013) 7, 074002 [arXiv:1307.5683 [hep-ph]].

[24] F. Beaujean, C. Bobeth and D. van Dyk, Eur. Phys. J. C **74** (2014) 2897 [arXiv:1310.2478 [hep-ph]].

[25] P. Biancofiore, P. Colangelo and F. De Fazio, Phys. Rev. D **89** (2014) 095018 [arXiv:1403.2944 [hep-ph]].

[26] P. Biancofiore, P. Colangelo, F. De Fazio and E. Scrimieri, arXiv:1408.5614 [hep-ph].

[27] A. J. Buras, F. De Fazio and J. Girrbach, JHEP **1302** (2013) 116 [arXiv:1211.1896 [hep-ph]].

[28] A. J. Buras and J. Girrbach, JHEP **1312** (2013) 009 [arXiv:1309.2466 [hep-ph]].

[29] A. J. Buras, D. Buttazzo, J. Girrbach-Noe and R. Knegjens, arXiv:1408.0728 [hep-ph].

[30] A. J. Buras, F. De Fazio and J. Girrbach-Noe, JHEP **1408** (2014) 039 [arXiv:1405.3850 [hep-ph]].

[31] A. J. Buras and J. Girrbach, Rept. Prog. Phys. **77** (2014) 086201 [arXiv:1306.3775 [hep-ph]].

[32] A. J. Buras, F. De Fazio and J. Girrbach, JHEP **1402** (2014) 112 [arXiv:1311.6729 [hep-ph], arXiv:1311.6729].

[33] A. J. Buras, F. De Fazio, J. Girrbach and M. V. Carlucci, JHEP **1302** (2013) 023 [arXiv:1211.1237 [hep-ph]].

[34] M. Papucci, K. Sakurai, A. Weiler and L. Zeune, arXiv:1402.0492 [hep-ph].

[35] A. Crivellin, J. Rosiek, P. H. Chankowski, A. Dedes, S. Jaeger and P. Tanedo, Comput. Phys. Commun. **184** (2013) 1004 [arXiv:1203.5023 [hep-ph]].

[36] W. Porod, Comput. Phys. Commun. **153** (2003) 275 [hep-ph/0301101].

[37] W. Porod and F. Staub, Comput. Phys. Commun. **183** (2012) 2458 [arXiv:1104.1573 [hep-ph]].

[38] D. M. Straub, JHEP **1308** (2013) 108 [arXiv:1302.4651, arXiv:1302.4651 [hep-ph]].